[redacted]

HYDRONAUTICS, incorporated
research in hydrodynamics

Research, consulting, and advanced engineering in the fields of NAVAL and INDUSTRIAL HYDRODYNAMICS. Offices and Laboratory in the Washington, D. C., area: Pindell School Road, Howard County, Laurel, Md.

HYDRONAUTICS, Incorporated

TECHNICAL REPORT 515-1

EXPERIMENTAL STUDY OF A CAVITY RUNNING BODY

By

T. T. Huang

September, 1965

Prepared Under

Bureau of Naval Weapons
Contract No. NOw-64-0306-c
and
Contract No. NOw-65-0344-c

TABLE OF CONTENTS

LIST OF FIGURES

NOTATION

A_b	Base area of the test nose
C_{Da}	Drag coefficient of the afterbody based on the nose base
$C_D = \frac{D_T + M}{\frac{1}{2}\rho U^2}$	Actual total drag coefficient
$C_D' = \frac{D_T}{\frac{1}{2}\rho U^2}$	Apparent total drag coefficient
$C_{DN} = \frac{D_N + M}{\frac{1}{2}\rho U^2}$	Actual nose drag coefficient
$C_{DN} = \frac{D_N}{\frac{1}{2}\rho U^2}$	Apparent nose drag coefficient
$C_{DN}(0)$	Actual nose drag at $\sigma_c = 0$
$C_{DN}(\sigma_c)$	Actual nose drag at finite cavity cavitation number σ_c
C_f	Skin-friction drag coefficient
C_{fN}	Skin-friction drag coefficient of the nose
C_{PN}	Pressure drag coefficient of the nose

$C_Q = \frac{Q}{UA_b}$	Air flow rate coefficient
$D = 2y_\infty$	Diameter of the half body at infinity downstream from the source point
D_T	Measured total drag force
D_N	Measured nose drag force
L	Length of the nose
M	Momentum thrust of the air ejected from the annular slot of the nose
m	Strength of source
p	Local pressure
p_c	Cavity pressure
p_v	Vapor pressure
p_∞	Free stream ambient pressure
Q	Ventilated air discharge at channel ambient pressure and $80^\circ F$
r	Distance from the source point to the stream surface of the source generated half body
U	Free stream velocity
x	Longitudinal axis

y	Radical ordinate from the axis of the half body of revolution
y_∞	Radius of half body base at infinity downstream from the source point
θ	Polar angle
ρ	Mass density of water
$\sigma = \frac{p_\infty - p_v}{\frac{1}{2}\rho U^2}$	Vapor cavitation number
$\sigma_c = \frac{p_\infty - p_c}{\frac{1}{2}\rho U^2}$	Cavity cavitation number

ABSTRACT

The results of an experimental investigation of a cavity running body are presented. The cavity running body consists of a blunt base nose of a half body of revolution and an afterbody which is completely enclosed by the ventilated cavity. Thus, the afterbody experiences almost no drag and the cavity drag due to the presence of the ventilated cavity becomes a very important component of the drag acting on the cavity running body. Theoretical and experimental results of every component of the drag of the cavity running body are presented and discussed. It is found that the total drag is almost independent of the vapor cavitation number but is highly dependent on the air flow rate to the cavity. The maximum drag reduction is 25 percent.

INTRODUCTION

In considering a streamlined body moving in water, nearly all of the resultant drag is associated with skin-friction. Consequently, in order to reduce the overall drag, the skin friction acting on the body must be reduced. One of the possible approaches is to produce slip between the water and the body by means of air lubrication.

Two schemes of air lubrication have been developed at HYDRONAUTICS, Incorporated. The first one is to produce a thin air film around the body, and the second one is to generate a steady ventilated cavity to enclose the body.

The first scheme attempts to maintain the lift force acting on the air-lubricated body comparable to that without air lubrication. Analytical study (1) has shown that if the air-film thickness is maintained within the order of one hundreth of an inch, the hydrodynamic force can be transmitted directly to the body through the thin air film. However, a previous experimental study (2) has encountered difficulties in achieving substantial stable thin film thicknesses with acceptable layer lengths. As a result, interest has turned to the second scheme, the cavity running body. Instead of injecting a thin air layer adjacent to the body, the second scheme is to generate a steady ventilated cavity to enclose a large portion of the body. This method reduces the instability of the air-water interface, but, since the cavity has essentially constant pressure, the buoyant force is lost. There is additional drag, which is called cavity drag, caused by the presence of the cavity. This drag may be significant in comparison with the skin-friction drag reduction. In order to provide a basis for assessing the merit of the cavity running performance, an experimental study was conducted.

In the present experiment, the air is pumped from the periphery of a blunt-base nose to form a steady cavity. An afterbody is attached to the nose base, which can be completely enclosed within the generated cavity and will have very little skin-friction drag. The blunt base nose is a half body of revolution which is generated mathematically by placing a point source in a uniform stream and by cutting the stream surface off at a finite

length in order to minimize the sum of the pressure and the skin-friction drag. The total force acting on the cavity running body consists of the skin-friction and the pressure drag of the nose, the cavity drag, the drag of the afterbody, and the momentum thrust of the ejected air. This report presents the experimental and theoretical results and a discussion of all these components of the drag on the cavity running body.

SELECTION OF NOSE SHAPE

In order to minimize the total drag of the cavity running body, it is necessary to select a nose of minimum drag. The nose drag consists of pressure, skin-friction, and cavity drag. The ventilated cavity drag of a blunt base body can not be estimated accurately and must be determined by experiment. However, it is possible to calculate the pressure and the skin-friction drag of a half body generated by a point source in a uniform stream. Therefore, the blunt base nose should be chosen as the half body which has the minimum sum of pressure and skin-friction drag. According to potential flow theory an infinitely long half body of revolution generated by a point source in a uniform stream has zero pressure drag, but its skin-friction drag is infinitely large, since it is infinitely long. If we compute the drag acting on the total surface from the tip to the downstream end of the half body with finite length, we find that the pressure drag decreases but the skin-friction increases with increasing length of the body. Thus, there is an optimum length of the half body which has the minimum sum of pressure and skin-friction drag.

The pressure distribution on the half body due to a point source of strength m located at the origin in a uniform stream is (Reference 3, p. 57):

$$p = p_\infty + \frac{\rho}{2} U^2 \left[\frac{3m^2}{16\pi^2 r^4 U^2} - \frac{m}{2\pi r^2 U} \right] \qquad [1]$$

where

$$r = \tfrac{1}{2} y_\infty \sec \frac{\theta}{2} \ , \quad y_\infty = \sqrt{\frac{m}{\pi U}} \ ,$$

r is the distance from the source point to the stream surface of the half body,

U is the free stream velocity,

p_∞ is the free stream ambient pressure,

θ is the polar angle, and

y_∞ is the radius of the body base at infinity downstream from the source point.

The pressure drag coefficient of the nose based on the base area at infinity downstream from the source point is

$$C_{PN} = \frac{2\pi}{\frac{1}{2}\rho U^2 \pi y_\infty^2} \int_0^y (p - p_\infty)\, y \, dy$$

$$= \int_0^\theta \left(3 \cos^5 \frac{\theta}{2} \sin \frac{\theta}{2} - 2 \cos^3 \frac{\theta}{2} \sin \frac{\theta}{2} \right) d\theta$$

$$= \cos^4 \frac{\theta}{2} - \cos^6 \frac{\theta}{2} \qquad [2]$$

where

$$y^2 = \frac{y_\infty^2}{2}(1 - \cos\theta), \text{ and}$$

y is the radial ordinate from the axis of the half body of revolution.

The skin-friction drag of the nose based on the base area at infinity downstream from the source point is

$$C_{fN} = \frac{C_f 2\pi}{\pi y_\infty^2} \int_{-y_\infty/2}^{x} y\, dx$$

$$= C_f \int_0^{\theta} \frac{\cos^2\theta + \cos\theta - 2}{1 + \cos\theta}\, d\theta$$

$$= C_f\left(\sin\theta - 2\tan\frac{\theta}{2}\right) \qquad [3]$$

where C_f is the skin-friction drag coefficient, which is a function of Reynolds number and which can be found elsewhere (Reference 4, p. 187).

The sum of $C_{PN} + C_{fN}$ and C_{PN} alone are plotted in Figure 1 for typical values of y_∞ and U. It is found that the minimum sum of the pressure and the skin-friction drag is at about L/D = 1.1, where L is the length of the body, and D is the diameter of the body base at infinity.

It was decided to use D equal to 4.5 inches and L equal to 6 inches for the present nose. The L/D of the nose selected is 1.33 which is slightly larger than the optimum value. The reason for using a slightly large L/D in this nose is that this nose has appreciably larger base area and its $C_{PN} + C_{fN}$ is still very close to the minimum value.

MODEL AND APPARATUS

The tests were conducted in the High Speed Water Channel at HYDRONAUTICS, Incorporated; a detailed description of this channel is presented in Reference 5. As shown in Figure 2, the model was supported by a 1-1/2 inch sting downstream from the model. The sting, in turn, was connected to a streamlined strut which was attached to the model support beam of the High Speed Water Channel. The model as shown in Figure 3 consisted of an aluminum nose and a wood afterbody which was coated with epoxy paint. A variable reluctance block gauge and a dummy block were installed inside the hollow of the afterbody. The positions of the block gauge and the dummy block were interchangable. The block gauge was used to measure the total drag of the nose and the afterbody when it was connected to the supporting sting. The drag of the nose was measured by interchanging the position of the dummy block and the block gauge which then was attached to the nose by a threaded shaft. A stilling chamber was formed by the void space inside the nose. The internal arrangement of the afterbody is shown in Figure 4.

The nose was 6 inches in length and 4.40 inches in diameter at its base. The stream surface of the nose was computed from

$$y = \sqrt{2.5312(1 - \cos \theta)} \qquad [4]$$

where θ is the polar angle and y is the radical distance in inches from the axis of symmetry to the surface of the nose. This was derived from potential theory for a point source in a uniform stream with the maximum value of y equal to 2.25 inches as θ approaches π.

The afterbody was formed by a cylinder 4.20 inches in diameter and 6 inches in length, which was tapered to a diameter of 2.10 inches in a distance of 10 inches by a parabola of third degree; the total length of the afterbody was 16 inches. The body was hollow so as to accommodate the installation of the block gauge, the dummy block, and the supporting sting. For convenience of installation, the afterbody was split into two pieces along the axis, and was connected together by three pairs of bolts. A fairing ring to smooth the step between the body and the sting was attached to the sting.

The air was supplied by an air compressor, which had a maximum capacity of 18 cfm at 150 psi. Two Fisher and Porter flowrators were used to measure the air supply rate, one with a maximum capacity of 19.6 cfm and the other with 6.25 cfm. Two

meters were necessary to span the wide flow rate range desired in the tests. A pressure regulator with pressure gauge and moisture filter was installed on the supply line upstream from the flowrator. At the junctions between the nose and the afterbody, and between the afterbody and the sting, two pairs of the tygon tubes were used to ensure that the supply line connections were flexible. This eliminated the possibility of transmitting drag through the supply lines (See Figure 5). The ventilating of air entered the stilling chamber from four air openings on the shaft which was connected to the supply lines. A hemispherical cap which formed a streamlined passage from the chamber to the slot opening for the air was attached to the shaft. The opening of the annular slot formed by the nose and the afterbody had a width of 0.084 inches. The air flow rate was regulated by the valves located at the downstream end of the flowrators.

A 1/16 inch pressure tap leading to the cavity region was located at the bottom of the middle section of the afterbody. A 1/4 inch tygon tube connected to the pressure tap. The cable of the block gauge, and the air supply line were led out through the sting, the strut, and the channel cover. The head difference between the cavity pressure and the channel pressure above the water was recorded by a manometer. The electrical output of the gauge was displayed by a digital counter.

A photographic view of the cavity running body being tested in the high speed channel is shown in Figure 6.

TEST PROCEDURE

At maximum channel speed the ventilated cavity could not enclose the afterbody at one atmosphere channel pressure. However, as the channel pressure was lowered to about two thirds of an atmosphere, the cavity was just large enough to enclose the afterbody. Therefore, it was decided to perform the tests on three channel speeds, 25, 30 and 33 fps, and two channel ambient pressures, 10 and 20 feet of water. These combinations of speed and channel ambient pressure covered a wide range of cavitation numbers from 0.58 to 1.42.

The overall test procedure was simple but systematic. The ventilated air flow rate was varied over the available range of the air compressor at each channel speed and ambient pressure. At a given channel speed, ambient pressure and ventilation air flow rate, the flowrator reading, block gauge reading, and cavity pressure were recorded. The channel water depth was maintained constant throughout the experiments. The axis of the model was set at 7.5 inches below the free surface and 7.5 inches above the channel floor. The pressure at the upstream end of the two flowrators was maintained at 60 psi for all the tests. The channel water temperature was recorded at regular intervals. The momentum thrust of the air ejected from the annular slot was measured at all test air flow rates and all test channel ambient pressures.

The test program was divided into two series: The first series was the measurements of the total drag of the nose and the afterbody and the second series was the measurement of the nose drag. The two series of tests were performed at identical test conditions.

RESULTS AND DISCUSSION

The accumulated data are reduced to four drag coefficients, two cavitation numbers and one ventilation air flow rate coefficient. The four drag coefficients are all referred to the base area of the nose, A_b. If D_T is the measured total drag force of the nose and the afterbody, D_N the measured drag force of the nose, M the momentum thrust of the air ejected from the slot, U the free stream velocity, and ρ the density of the water the actual total drag coefficient, C_D, is defined by $C_D = (D_T + M)/\frac{1}{2}\rho U^2 A_b$ and the apparent total drag coefficient, C_D', by $C_D' = D_T/\frac{1}{2}\rho U^2 A_b$, and the actual nose drag coefficient, C_{DN}, is defined by $C_{DN} = (D_N + M)/\frac{1}{2}\rho U^2 A_b$, and the apparent nose drag coefficient, C_{DN}', by $C_{DN}' = D_N/\frac{1}{2}\rho U^2 A_b$. It is important to note that the actual drag of the body is equal to the sum of the measured drag and the momentum thrust of the air. Two different cavitation numbers are vapor cavitation number, $\sigma = (p_\infty - p_v)/\frac{1}{2}\rho U^2$; and cavity cavitation number, $\sigma_c = (p_\infty - p_c)/\frac{1}{2}\rho U^2$. Here p_∞ is the ambient uniform stream pressure, p_v the vapor pressure, and p_c the cavity pressure. The air flow rate coefficient C_Q is defined as $C_Q = Q/UA_b$, where Q is the ventilation air discharge rate at channel ambient pressure and $80^\circ F$.

The results are plotted as drag coefficient versus air flow rate coefficient with vapor cavitation number as the parameter, in Figures 7 through 10. It is important to note that the total and nose drag coefficients are almost identical for every given test condition. Thus, the afterbody experiences almost no drag at any test condition. In addition, as long as the afterbody is properly enclosed by the ventilated cavity, the drag coefficient is almost independent of vapor cavitation number, but is highly dependent on the cavity cavitation number which, in turn, is a function of the air flow rate.

As can be seen from Figures 7 and 8, both the actual total and nose drag coefficients, C_D and C_{DN}, decrease with the increase of air flow rate coefficient C_Q. Both C_D and C_{DN} seem to approach an asymptotic value at large values of C_Q. As shown in Figure 7, the actual total drag coefficient at $C_Q = 0$, extended from the experimental curve is identical to the theoretical C_D without ventilation. The theoretical C_D is computed from the sum of pressure and skin-friction drag of the nose and the skin-friction drag of the afterbody. However, the measured C_D without ventilation is slightly larger than the theoretical C_D. This difference is probably caused by the formation of eddies at the abrupt transition between the nose and the afterbody. The nose drag without ventilation was so large it could not be measured with the block gauge used.

The apparent total and nose drag coefficients, C_D and C_{DN}, decrease rapidly with increasing air flow rate coefficient C_Q as shown in Figures 9 and 10. This is due to the contribution of

the momentum thrust of the ventilated air ejected from the annular slot, which increases with C_Q.

The total drag reduction is shown in Figure 11. Within the test range of air flow coefficient, the total drag reduction increases almost linearly with increasing C_Q. The maximum total drag reduction obtained is 25 percent. C_D, the actual total drag coefficient of the cavity running body can be written as

$$C_D = C_{PN} + C_{fN} + C_{Da} + \sigma_c \qquad [5]$$

where C_{PN} is the pressure drag coefficient and C_{fN} is the skin-friction drag coefficient of the nose, C_{Da} the drag coefficient of the afterbody, and σ_c is the cavity cavitation number, if all the drag coefficients are referred to the base area of the nose. Since we found that C_{Da} is negligibly small so long as the afterbody is properly enclosed by the ventilated cavity, the actual total and nose drag coefficients are identical, i.e.,

$$C_D \simeq C_{DN} = C_{PN} + C_{fN} + \sigma_c \qquad [6]$$

According to the analysis, the sum of C_{PN} and C_{fN} is found to be 0.02. The value of $C_{DN}/(C_{PN} + C_{fN} + \sigma_c)$ should be equal to unity. The experimental results are shown in Figure 12, and good agreement between the analysis and experiment is obtained. The effect

of σ_c on the drag of the cavity running body, according to the experimental results shown in Figure 13, is

$$C_{DN}(\sigma_c) = C_{DN}(0) + \sigma_c$$

where $C_{DN}(0)$ is the actual nose drag at $\sigma_c = 0$ and $C_{DN}(0)$ is equal to the sum of pressure and skin-friction drag coefficients of the test nose and was found to be 0.02. This result is in good agreement with the approximate theory of Armstrong (6). It is important to note that the cavity cavitation number is a large component of the nose drag.

The dependence of cavity cavitation number on the air flow rate coefficient C_Q is shown in Figure 14. It can be seen that σ_c decreases almost linearly with increasing C_Q. However, the trailing end of the cavity was disturbed by the model supporting sting and strut, so no measurement of cavity shape was attempted in this study. It was found during the test that the maximum vapor cavitation number which enables the ventilated cavity to enclose the afterbody properly with the small test range of supply air is about 1.5.

CONCLUSION

As long as the afterbody is properly enclosed by the ventilated cavity, the afterbody experiences almost no drag, and the drag coefficients are almost independent of vapor cavitation number but are highly dependent on the air flow rate to the cavity.

The maximum vapor cavitation number for the ventilated cavity to enclose the afterbody properly with the small test range of supply air is about 1.5.

Within the test range of air supply, the percentage of the total drag reduction increases almost linearly with the increasing air flow rate. The maximum total drag reduction obtained was 25 percent.

The actual total and nose drag coefficients are almost identical at every condition; they are equal to the sum of the pressure drag and skin-friction drag of the nose and the cavity cavitation number. The effect of cavity cavitation number σ_c on the drag of the cavity running body is found to be

$$C_{DN}(\sigma_c) = C_{DN}(0) + \sigma_c$$

Thus, the cavity cavitation number is the major component of the drag of the cavity running body.

Within the test range, the cavity cavitation number decreases almost linearly with the increase of air flow rate coefficient.

REFERENCES

1. Pao, Y. H., "Viscous Flow Along a Surface with Gas Lubrication," HYDRONAUTICS, Incorporated Technical Report 007-02, August, 1961.

2. Stoller, H. M., "Experimental Investigation of Gas Lubricated Water Boundary Layers," HYDRONAUTICS, Incorporated Technical Report 007-03, May 1963.

3. Streeter, V. L., Fluid Dynamics, McGraw-Hill Book Company, Incorporated, 1948.

4. Rouse, H., Elementary Mechanics of Fluids, John Wiley and Sons, Inc., 1946.

5. Johnson, V. E., Jr., and Goodman, A., "The HYDRONAUTICS, Incorporated Variable-Pressure Free-Surface, High-Speed Channel," HYDRONAUTICS, Incorporated Technical Report 229-1, April 1964.

6. Armstrong, A. H., "Drag Coefficients of Wedge and Cones in Cavity Flow," Armament Research Establishment, Report 21/54, Ft. Halstead, Kent, England, 1954.

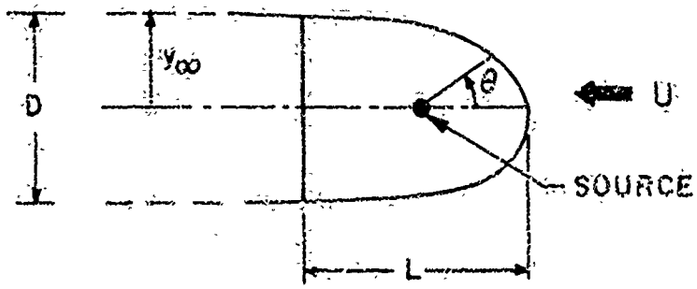

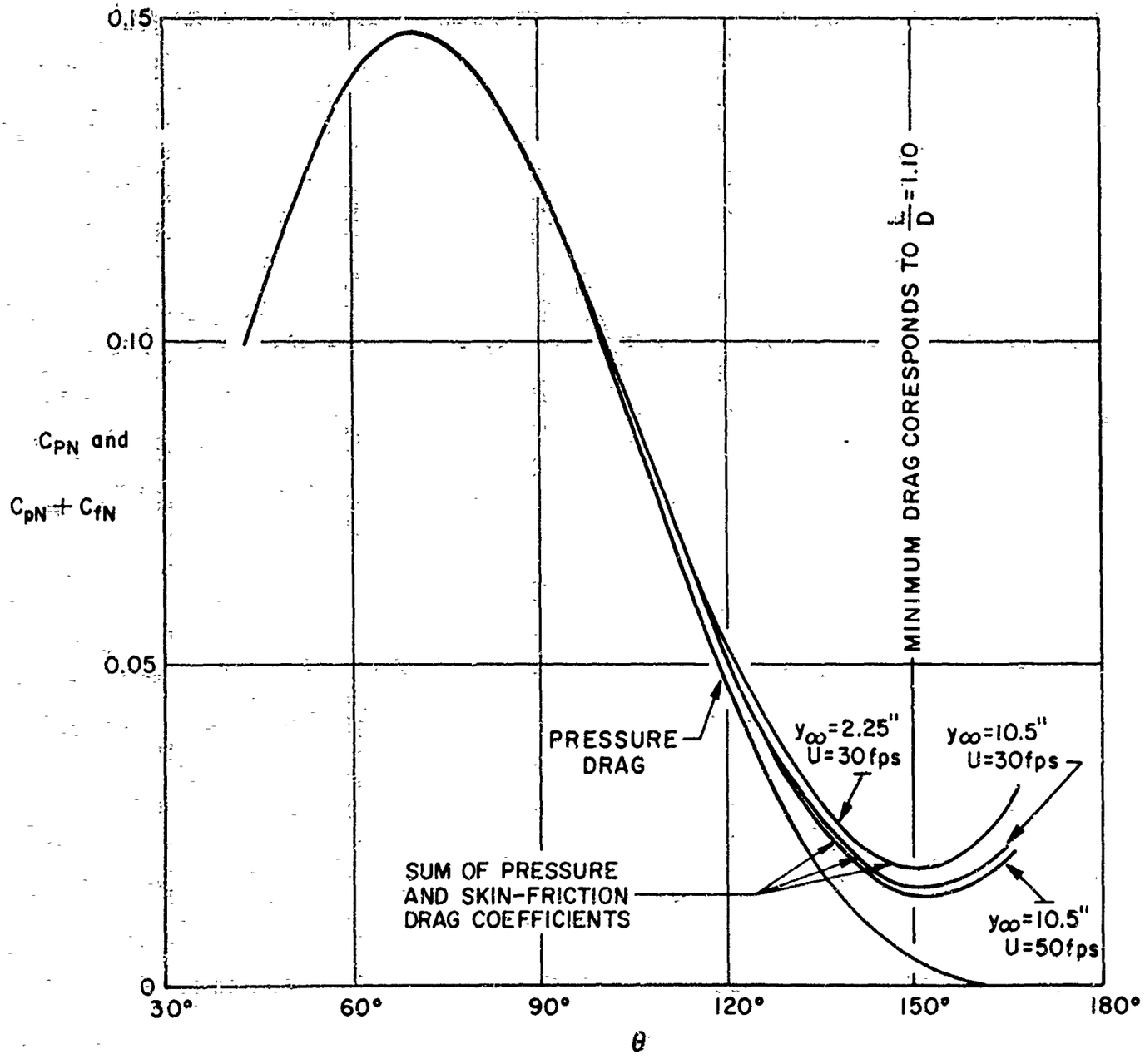

FIGURE 1—DRAG PROFILE COEFFICIENT OF A SOURCE GENERATED BODY

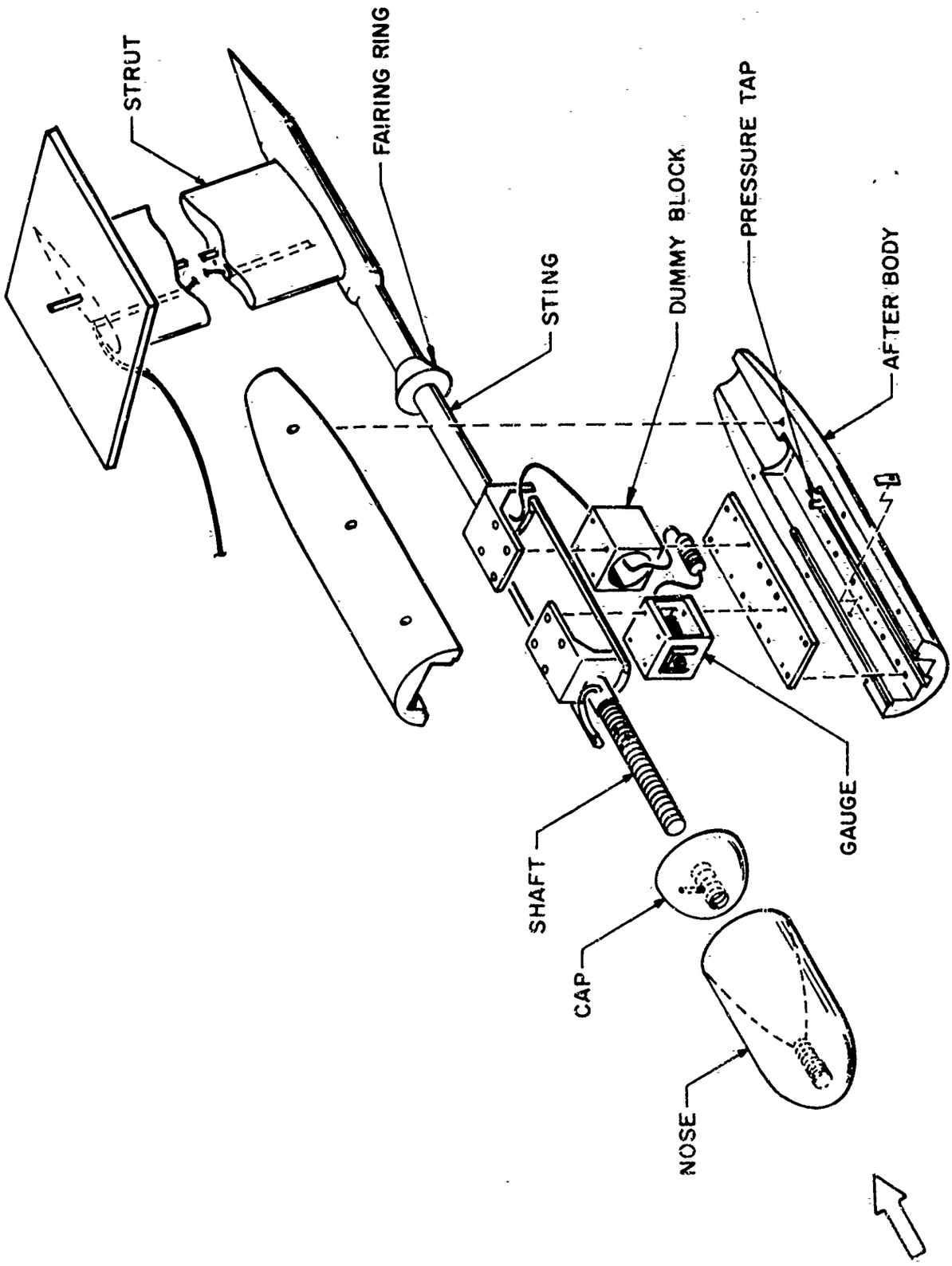

FIGURE 2-SCHEMATIC OF THE TEST CONFIGURATION OF THE CAVITY RUNNING BODY

FIGURE 3 – PHOTOGRAPHIC VIEW OF THE SHAPE OF THE CAVITY RUNNING BODY

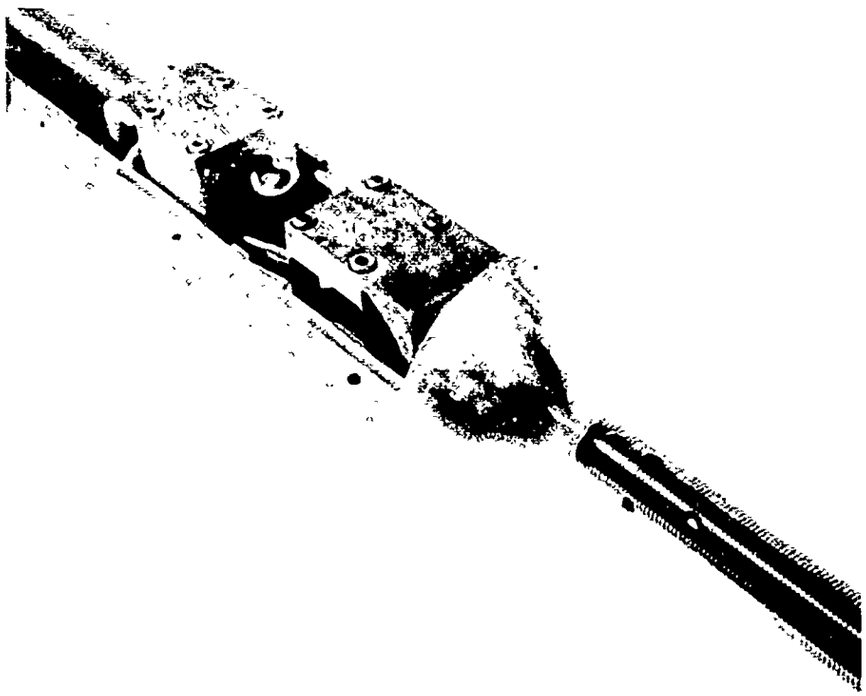

FIGURE 4 -- INTERNAL ARRANGEMENT OF THE AFTERBODY

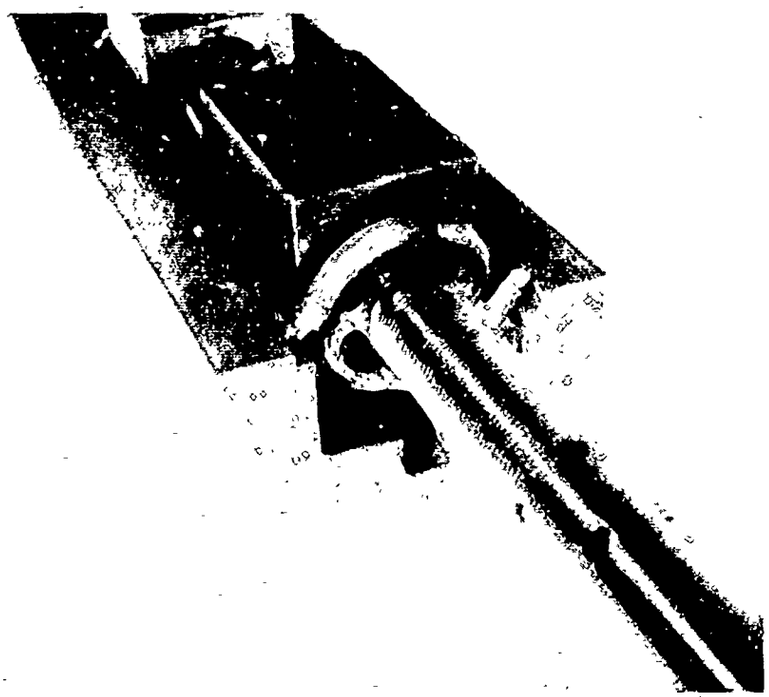

FIGURE 5 -- THE FLEXIBLE CONNECTIONS OF THE AIR SUPPLY LINES

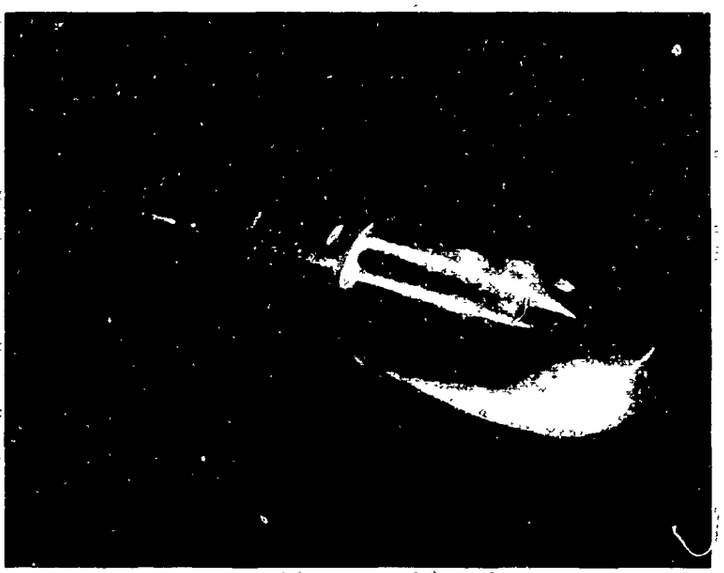

FIGURE 6—THE MODEL TESTED IN THE HIGH SPEED WATER CHANNEL

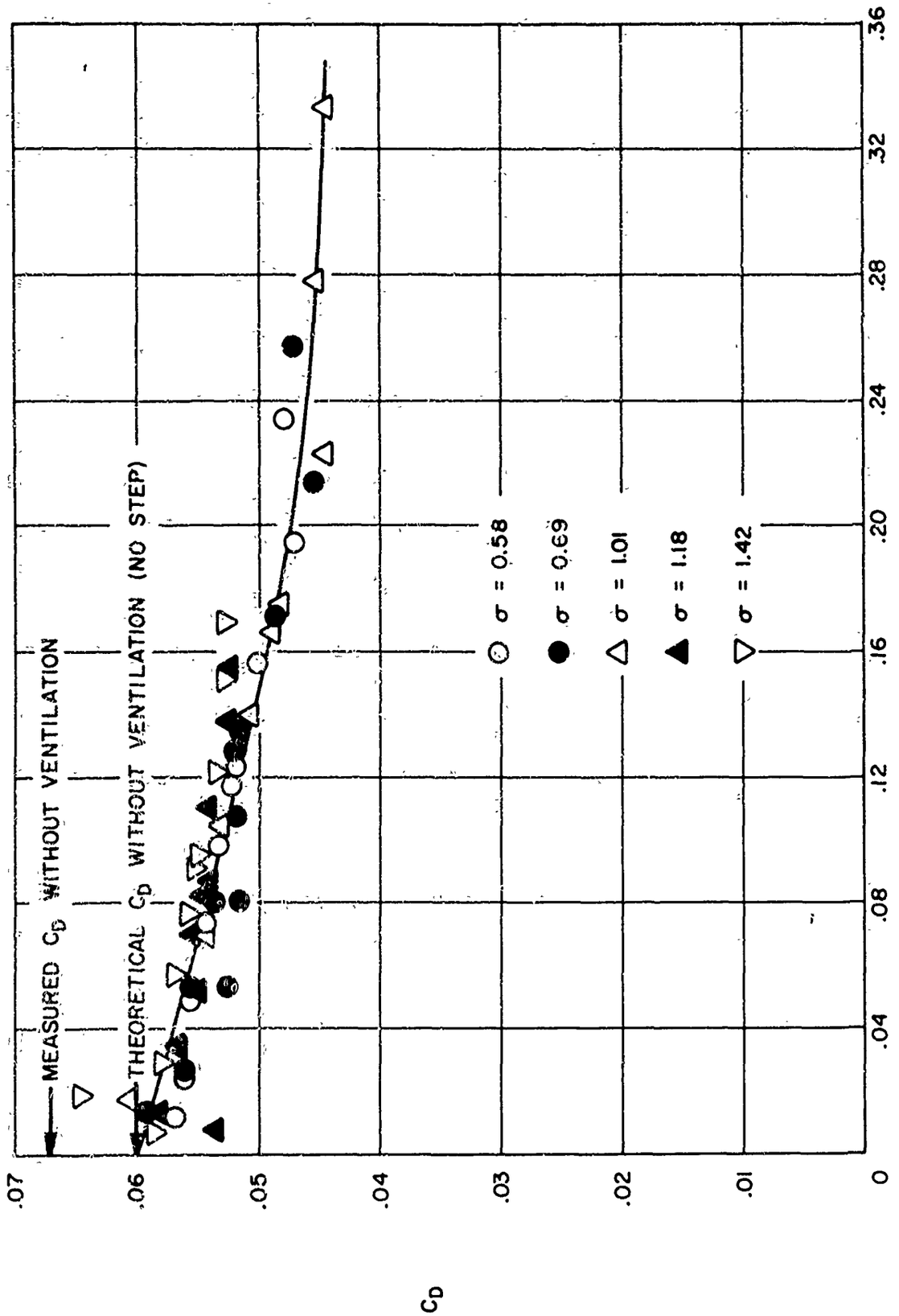

FIGURE 7—VARIATION OF ACTUAL TOTAL DRAG COEFFICIENT WITH AIR FLOW RATE COEFFICIENT

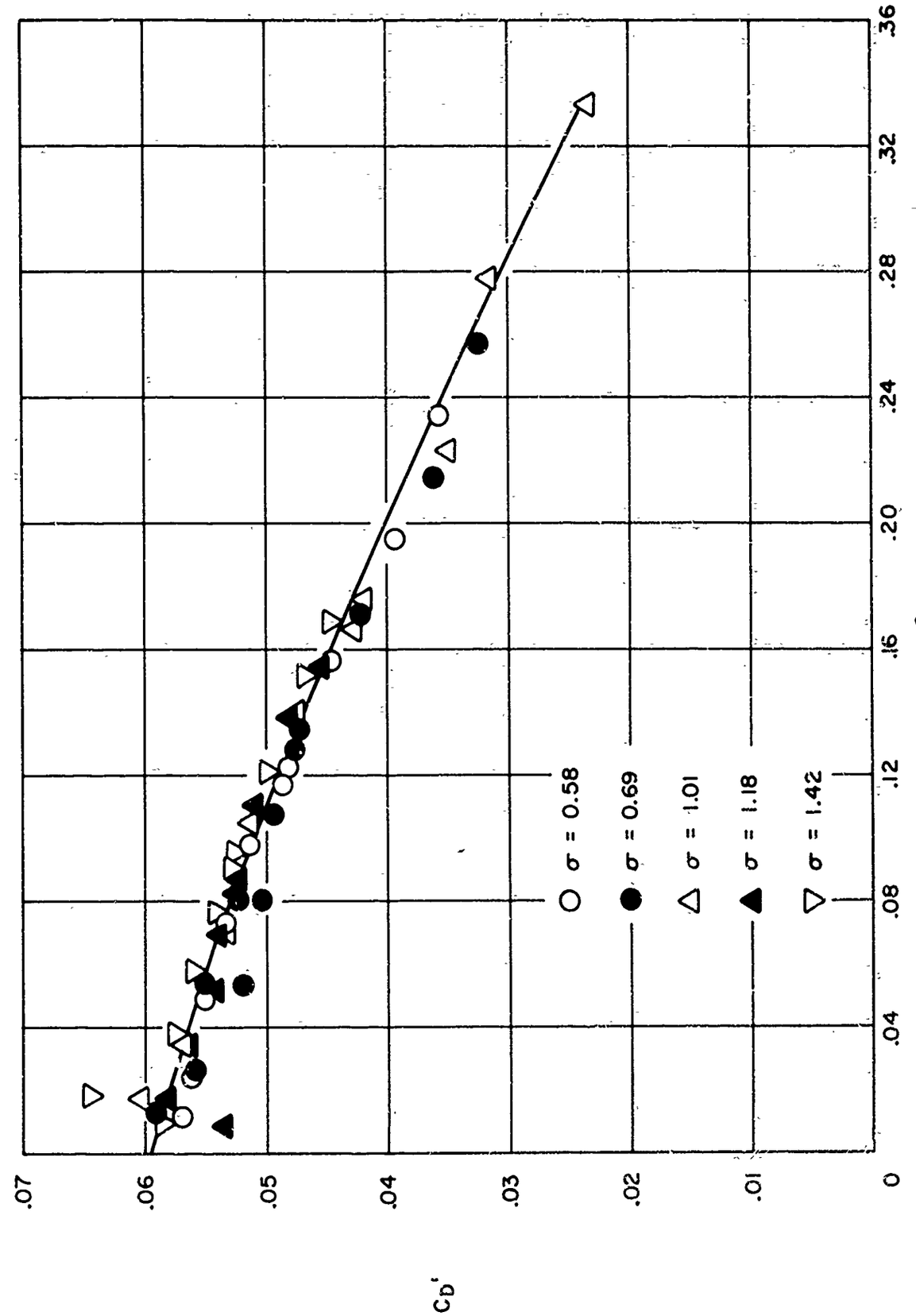

FIGURE 9—VARIATION OF APPARENT TOTAL DRAG COEFFICIENT WITH AIR FLOW RATE COEFFICIENT

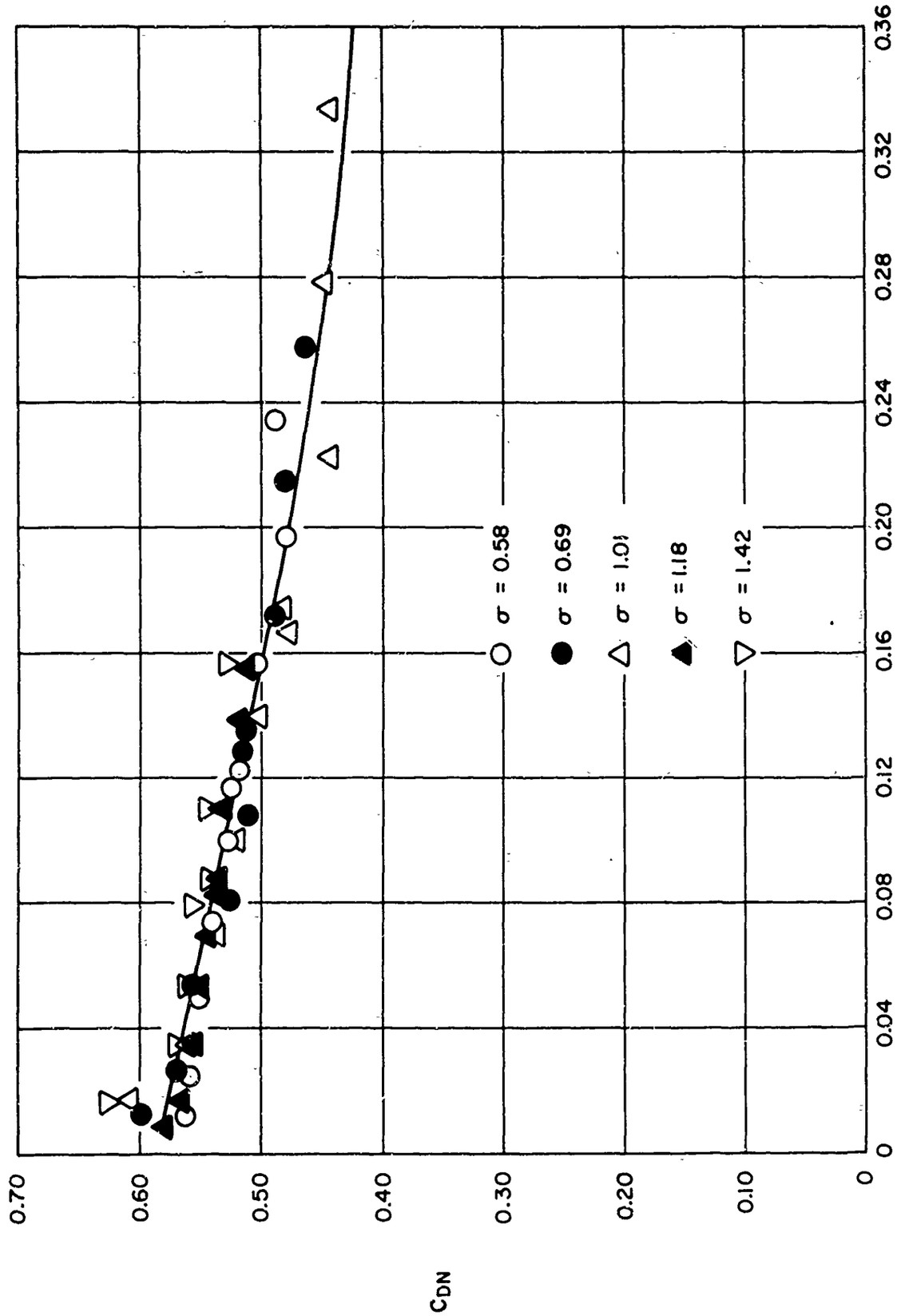

FIGURE 8–VARIATION OF ACTUAL NOSE DRAG COEFFICIENT WITH AIR FLOW RATE COEFFICIENT

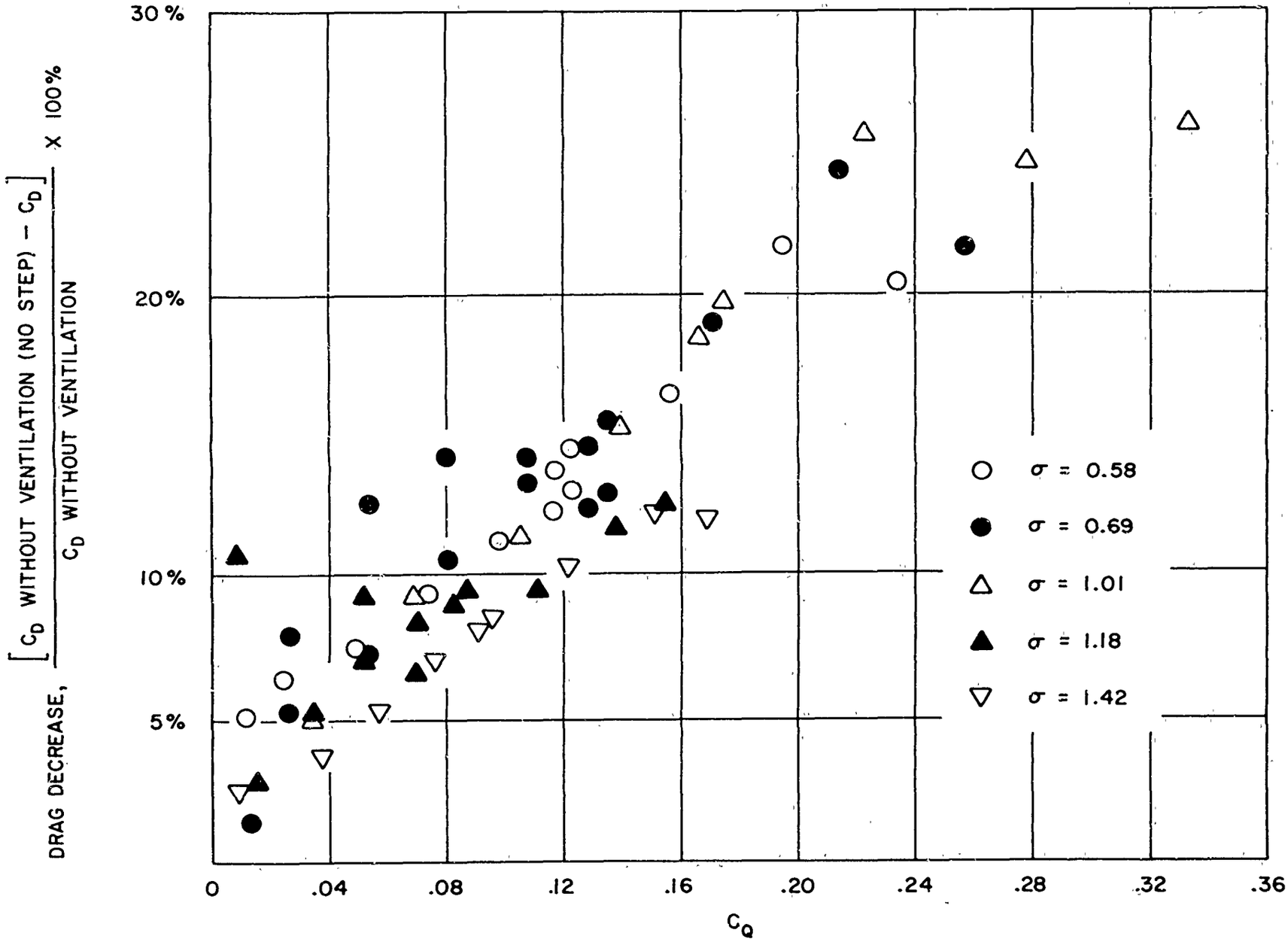

FIGURE 11—TOTAL DRAG REDUCTION

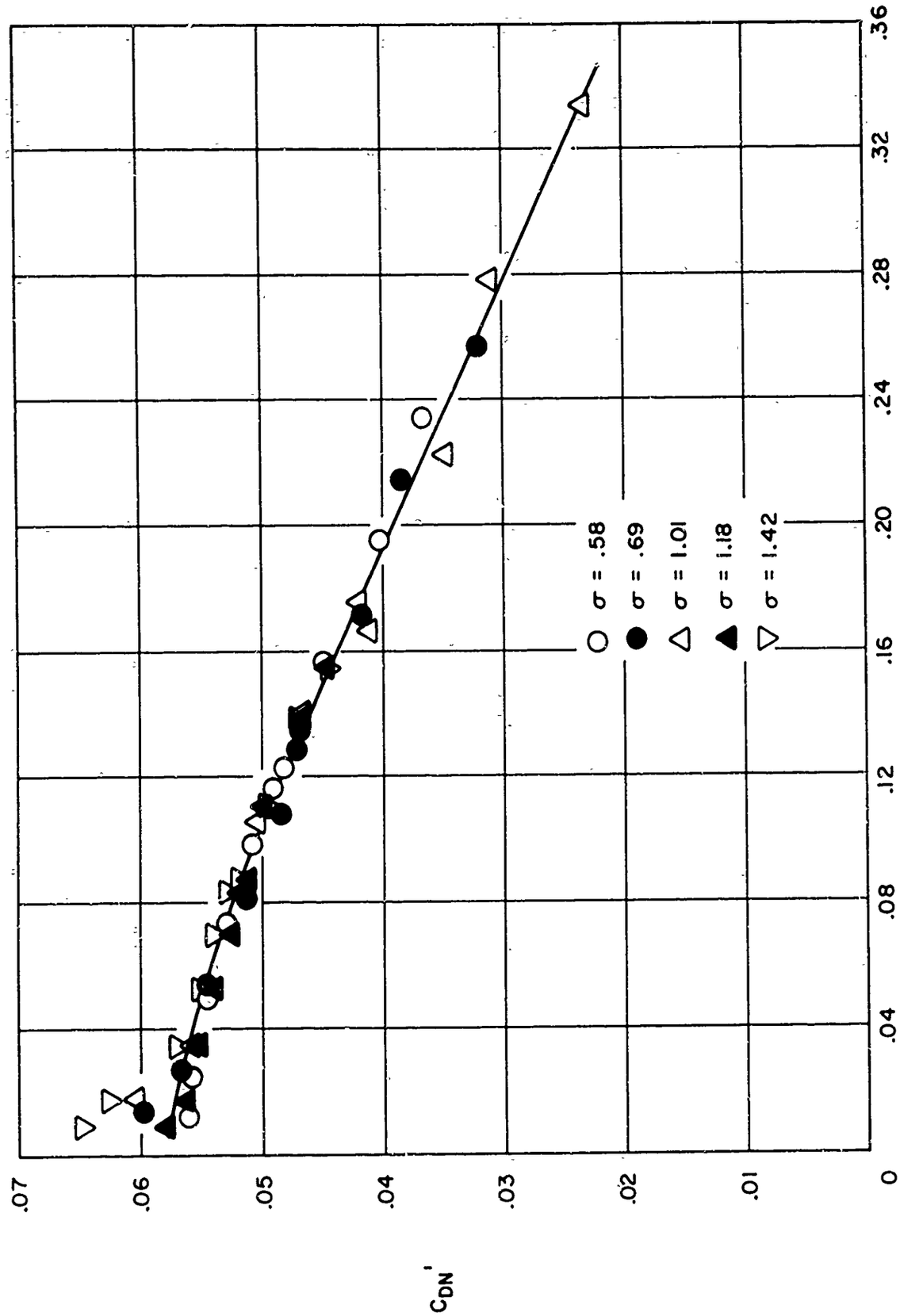

FIGURE 10–VARIATION OF APPARENT NOSE DRAG COEFFICIENT WITH AIR FLOW RATE COEFFICIENT

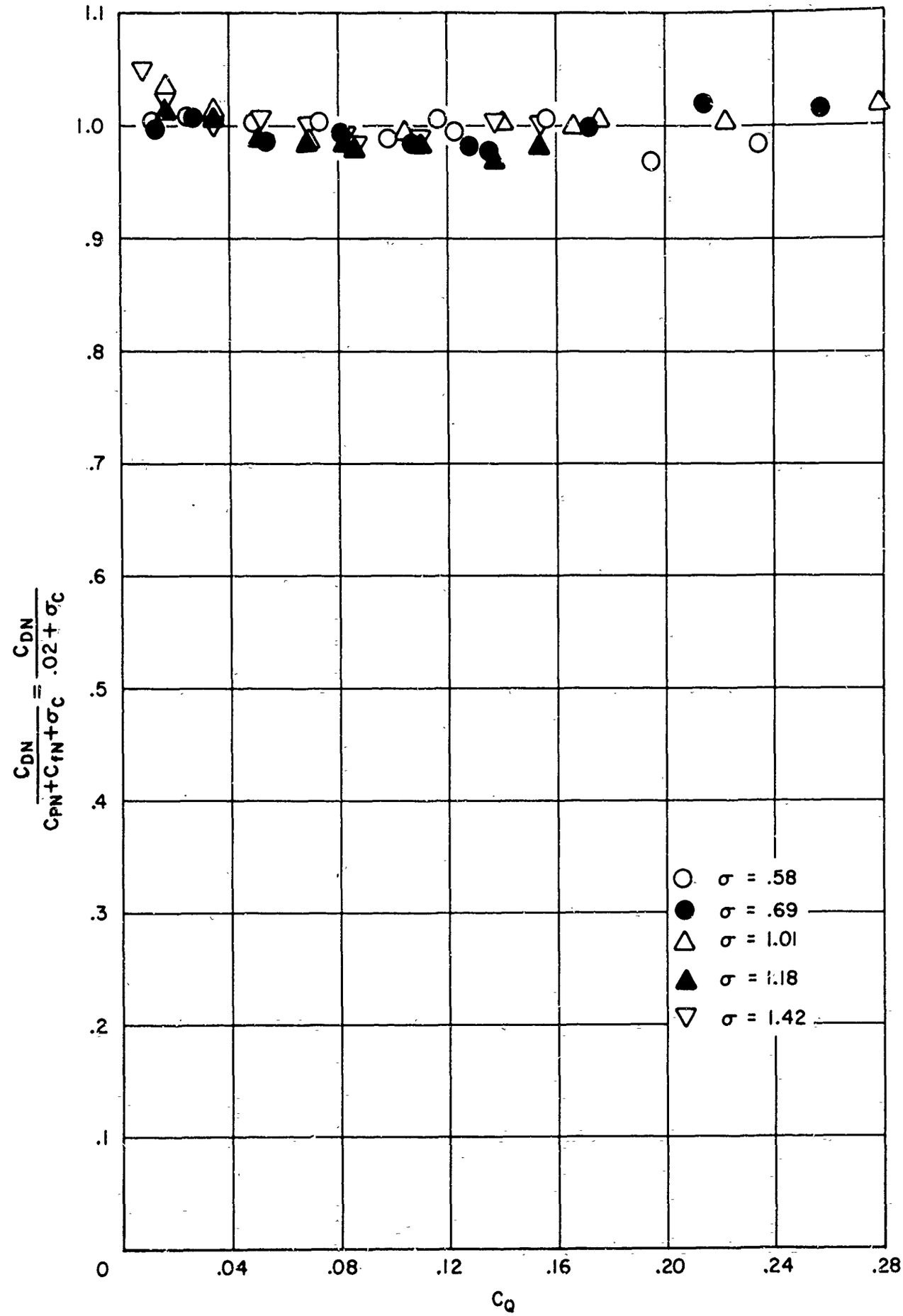

FIGURE 12-COMPARISON OF NOSE DRAG COMPONENTS

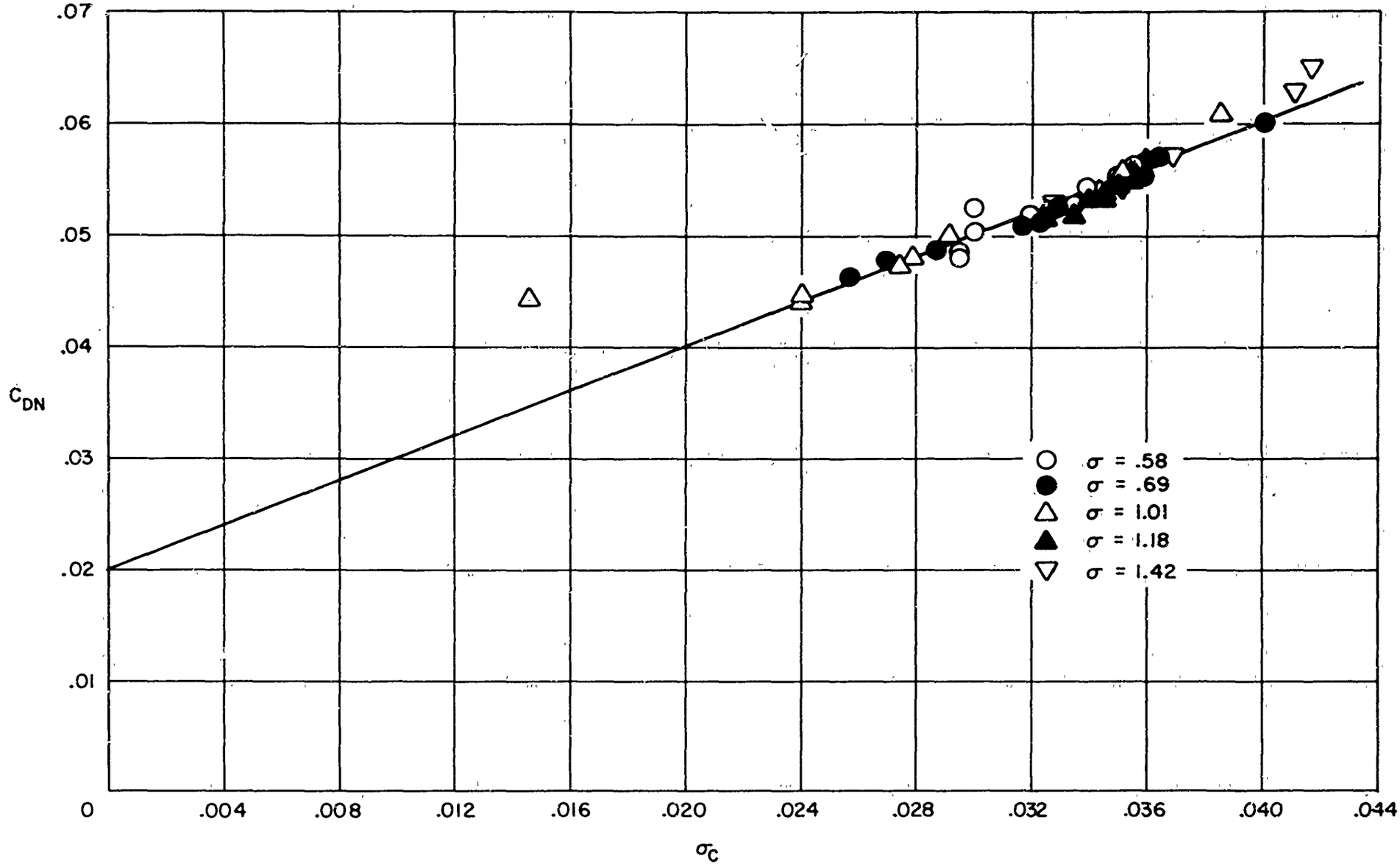

FIGURE 13—VARIATION OF ACTUAL NOSE DRAG COEFFICIENT WITH CAVITY CAVITATION NUMBER

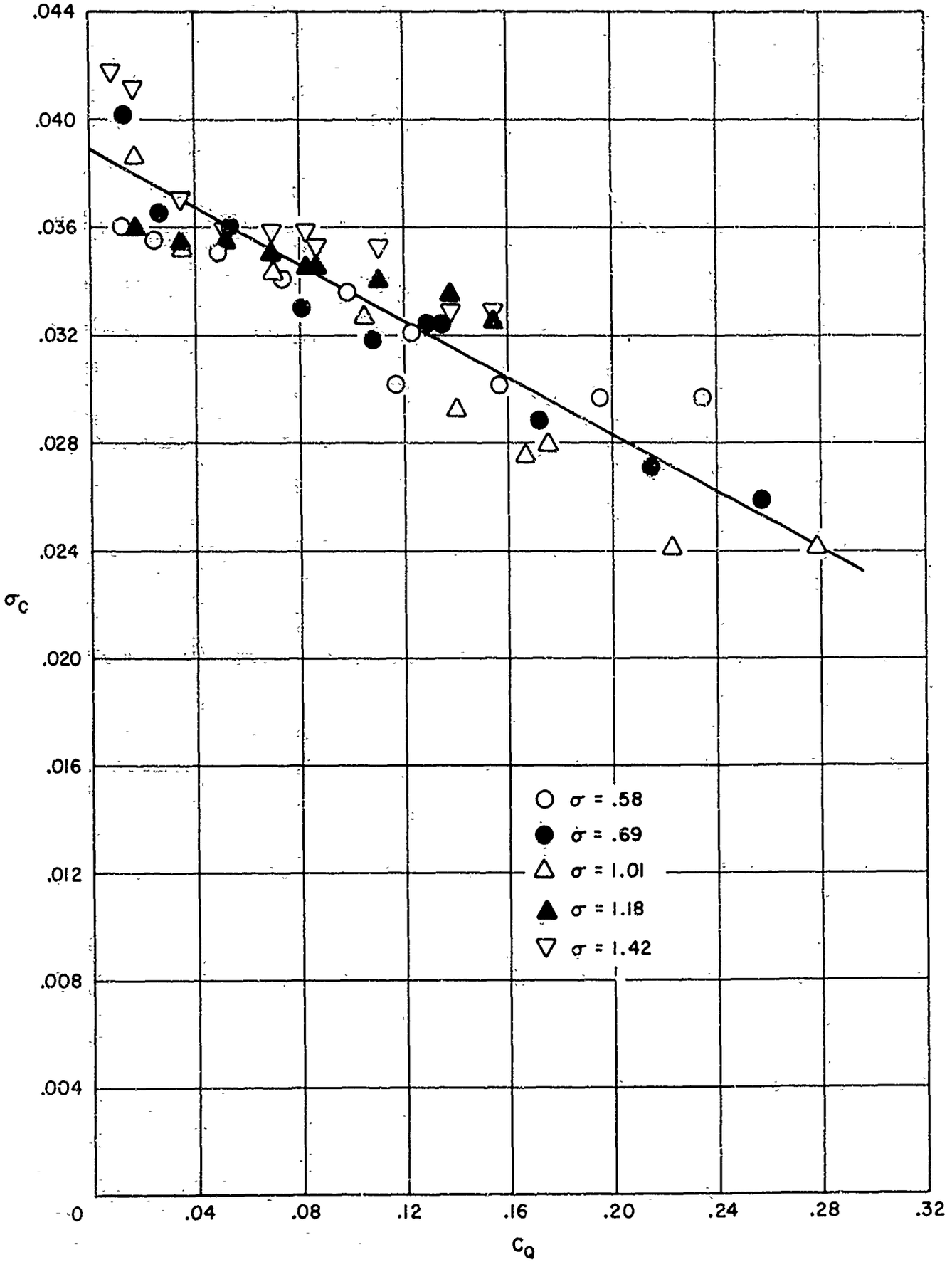

FIGURE 14—VARIATION OF CAVITY CAVITATION NUMBER WITH AIR FLOW RATE COEFFICIENT

UNCLASSIFIED

Security Classification

DOCUMENT CONTROL DATA - R&D

(Security classification of title, body of abstract and indexing annotation must be entered when the overall report is classified)

1. ORIGINATING ACTIVITY (Corporate author)
HYDRONAUTICS, Incorporated
Pindell School Road, Howard County,
Laurel, Maryland

2a. REPORT SECURITY CLASSIFICATION
UNCLASSIFIED

2b. GROUP

3. REPORT TITLE

EXPERIMENTAL STUDY OF A CAVITY RUNNING BODY

4. DESCRIPTIVE NOTES (Type of report and inclusive dates)
Technical Report

5. AUTHOR(S) (Last name, first name, initial)

Huang, T. T.

6. REPORT DATE	7a. TOTAL NO. OF PAGES	7b. NO. OF REFS
September 1965	34	6

8a. CONTRACT OR GRANT NO.	9a. ORIGINATOR'S REPORT NUMBER(S)
NOw-64-0306-c and NOw-65-0344-c b. PROJECT NO.	Technical Report 515-1
c.	9b. OTHER REPORT NO(S) (Any other numbers that may be assigned this report)
d.	

10. AVAILABILITY/LIMITATION NOTICES

Qualified requesters may obtain copies of this report from DDC.

DISTRIBUTION OF THIS DOCUMENT IS UNLIMITED

11. SUPPLEMENTARY NOTES	12. SPONSORING MILITARY ACTIVITY
	Bureau of Naval Weapons

13. ABSTRACT

The results of an experimental investigation of a cavity running body are presented. The cavity running body consists of a blunt base nose of a half body of revolution and an afterbody which is completely enclosed by the ventilated cavity. Thus, the afterbody experiences almost no drag and the cavity drag due to the presence of the ventilated cavity becomes a very important component of the drag acting on the cavity running body. Theoretical and experimental results of every component of the drag of the cavity running body are presented and discussed. It is found that the total drag is almost independent of the vapor cavitation number but is highly dependent on the air flow rate to the cavity. The maximum drag reduction is 25 percent.

UNCLASSIFIED

Security Classification

14. KEY WORDS	LINK A		LINK B		LINK C	
	ROLE	WT	ROLE	WT	ROLE	WT
[illegible] city [illegible] city [illegible]						

INSTRUCTIONS

1. ORIGINATING ACTIVITY: Enter the name and address of the contractor, subcontractor, grantee, Department of Defense activity or other organization *(corporate author)* issuing the report.

2a. REPORT SECURITY CLASSIFICATION: Enter the overall security classification of the report. Indicate whether "Restricted Data" is included. Marking is to be in accordance with appropriate security regulations.

2b. GROUP: Automatic downgrading is specified in DoD Directive 5200.10 and Armed Forces Industrial Manual. Enter the group number. Also, when applicable, show that optional markings have been used for Group 3 and Group 4 as authorized.

3. REPORT TITLE: Enter the complete report title in all capital letters. Titles in all cases should be unclassified. If a meaningful title cannot be selected without classification, show title classification in all capitals in parenthesis immediately following the title.

4. DESCRIPTIVE NOTES: If appropriate, enter the type of report, e.g., interim, progress, summary, annual, or final. Give the inclusive dates when a specific reporting period is covered.

5. AUTHOR(S): Enter the name(s) of author(s) as shown on or in the report. Enter last name, first name, middle initial. If military, show rank and branch of service. The name of the principal author is an absolute minimum requirement.

6. REPORT DATE: Enter the date of the report as day, month, year; or month, year. If more than one date appears on the report, use date of publication.

7a. TOTAL NUMBER OF PAGES: The total page count should follow normal pagination procedures, i.e., enter the number of pages containing information.

7b. NUMBER OF REFERENCES: Enter the total number of references cited in the report.

8a. CONTRACT OR GRANT NUMBER: If appropriate, enter the applicable number of the contract or grant under which the report was written.

8b, 8c, & 8d. PROJECT NUMBER: Enter the appropriate military department identification, such as project number, subproject number, system numbers, task number, etc.

9a. ORIGINATOR'S REPORT NUMBER(S): Enter the official report number by which the document will be identified and controlled by the originating activity. This number must be unique to this report.

9b. OTHER REPORT NUMBER(S): If the report has been assigned any other report numbers *(either by the originator or by the sponsor)*, also enter this number(s).

10. AVAILABILITY/LIMITATION NOTICES: Enter any limitations on further dissemination of the report, other than those imposed by security classification, using standard statements such as:

(1) "Qualified requesters may obtain copies of this report from DDC."

(2) "Foreign announcement and dissemination of this report by DDC is not authorized."

(3) "U. S. Government agencies may obtain copies of this report directly from DDC. Other qualified DDC users shall request through _____."

(4) "U. S. military agencies may obtain copies of this report directly from DDC. Other qualified users shall request through _____."

(5) "All distribution of this report is controlled. Qualified DDC users shall request through _____."

If the report has been furnished to the Office of Technical Services, Department of Commerce, for sale to the public, indicate this fact and enter the price, if known.

11. SUPPLEMENTARY NOTES: Use for additional explanatory notes.

12. SPONSORING MILITARY ACTIVITY: Enter the name of the departmental project office or laboratory sponsoring *(paying for)* the research and development. Include address.

13. ABSTRACT: Enter an abstract giving a brief and factual summary of the document indicative of the report, even though it may also appear elsewhere in the body of the technical report. If additional space is required, a continuation sheet shall be attached.

It is highly desirable that the abstract of classified reports be unclassified. Each paragraph of the abstract shall end with an indication of the military security classification of the information in the paragraph, represented as *(TS), (S), (C), or (U)*.

There is no limitation on the length of the abstract. However, the suggested length is from 150 to 225 words.

14. KEY WORDS: Key words are technically meaningful terms or short phrases that characterize a report and may be used as index entries for cataloging the report. Key words must be selected so that no security classification is required. Identifiers, such as equipment model designation, trade name, military project code name, geographic location, may be used as key words but will be followed by an indication of technical context. The assignment of links, roles, and weights is optional.